

Supplementary material for LHCb-PAPER-2017-019

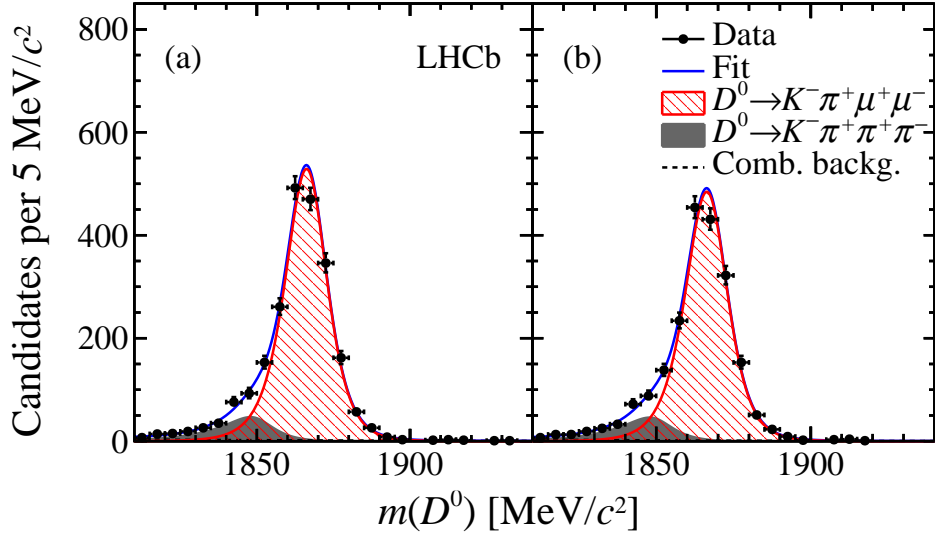


Figure 4: Distributions of $m(D^0)$ for the $D^0 \rightarrow K^- \pi^+ [\mu^+ \mu^-]_{\rho^0/\omega}$ decays resulting from the selection optimized for (a) $D^0 \rightarrow \pi^+ \pi^- \mu^+ \mu^-$ and (b) $D^0 \rightarrow K^+ K^- \mu^+ \mu^-$ signals, with fit projections overlaid.

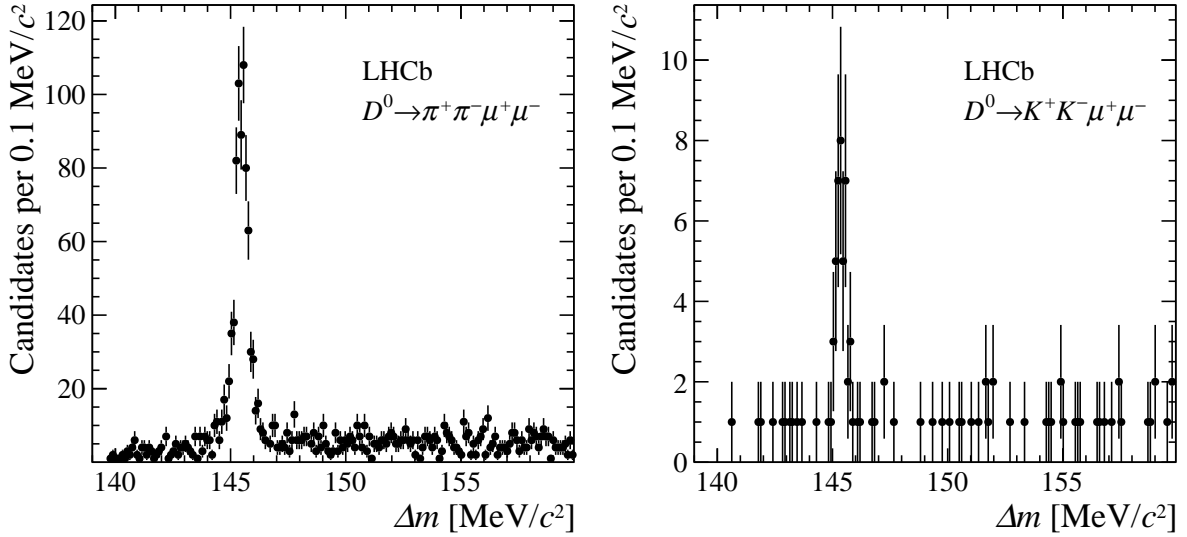


Figure 5: Distributions of Δm for (left) $D^0 \rightarrow \pi^+ \pi^- \mu^+ \mu^-$ and (right) $D^0 \rightarrow K^+ K^- \mu^+ \mu^-$ signals. Additionally to the selection explained in the main text, only candidates with D^0 mass in the range $1840 - 1890 \text{ MeV}/c^2$ are shown.

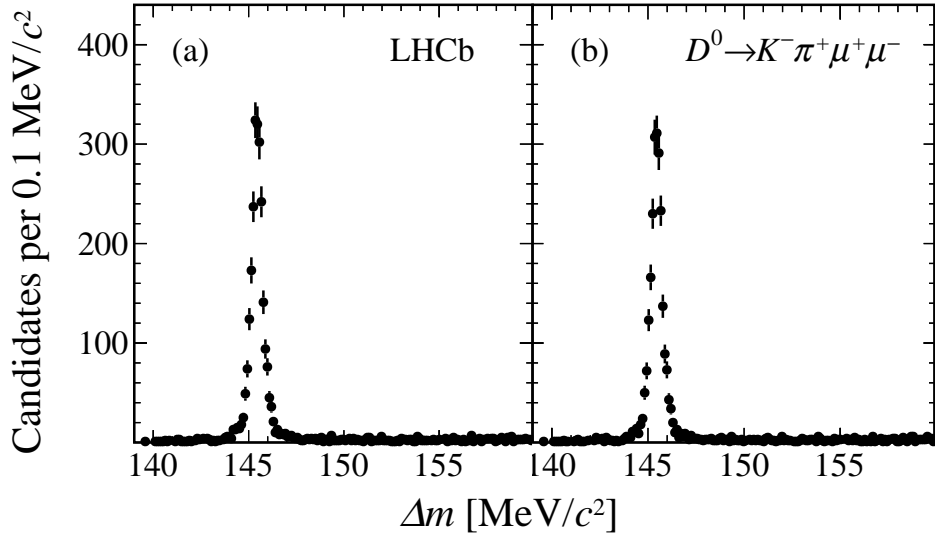


Figure 6: Distributions of Δm for the $D^0 \rightarrow K^- \pi^+ [\mu^+ \mu^-]_{\rho^0/\omega}$ decays resulting from the selection optimized for (a) $D^0 \rightarrow \pi^+ \pi^- \mu^+ \mu^-$ and (b) $D^0 \rightarrow K^+ K^- \mu^+ \mu^-$ signals. Additionally to the selection explained in the main text, only candidates with D^0 mass in the range 1840–1890 MeV/c^2 are shown.

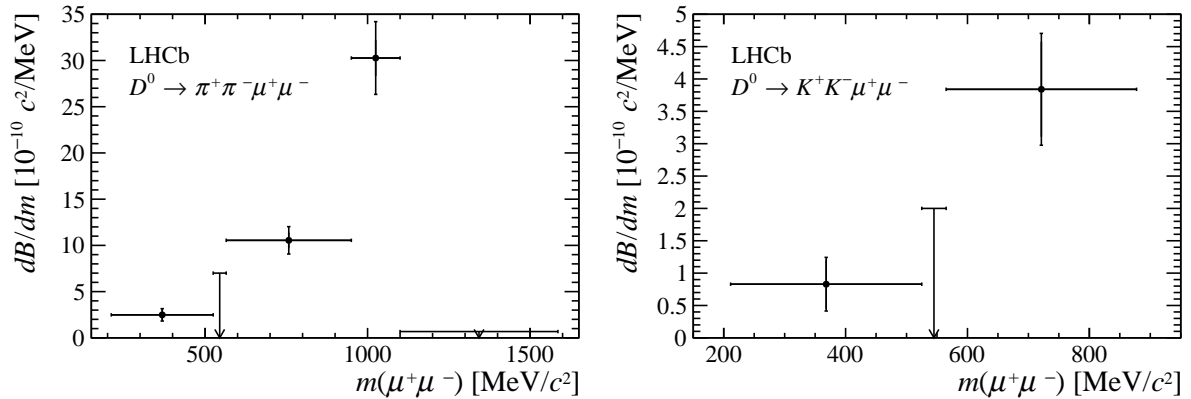


Figure 7: Differential branching fraction as a function of the dimuon mass for (left) $D^0 \rightarrow \pi^+ \pi^- \mu^+ \mu^-$ and (right) $D^0 \rightarrow K^+ K^- \mu^+ \mu^-$ decays. The arrows represent the upper limits at 95% confidence level.